A QUANTUM ALGORITHM FOR LINEAR PDES ARISING IN FINANCE

FILIPE FONTANELA, ANTOINE JACQUIER, AND MUGAD OUMGARI

Abstract. We propose a hybrid quantum-classical algorithm, originated from quantum chemistry, to price European and Asian options in the Black-Scholes model. Our approach is based on the equivalence between the pricing partial differential equation and the Schrödinger equation in imaginary time. We devise a strategy to build a shallow quantum circuit approximation to this equation, only requiring few qubits. This constitutes a promising candidate for the application of Quantum Computing techniques (with large number of qubits affected by noise) in Quantitative Finance.

1. Introduction

Pricing financial derivatives accurately and efficiently is one of the most difficult and exciting challenges in Mathematical Finance. While the existence of closed-form solutions are known in very few simple cases, the vast majority of models do not admit one, and computing derivatives rely on computational techniques, either using Monte Carlo simulation methods or via numerical methods for partial differential equations, such as finite differences or finite elements. Unfortunately, these techniques can rapidly become computationally intensive when the model becomes complicated, or when the dimension of the problem (in the case of Basket options for example) becomes large. While huge progress has been made over the past decades, these techniques have inherent limitations which cannot be overcome when run on classical computers.

Recently, the emergence of small-scale quantum computers has caught the eyes of mathematicians and financial engineers [15, 9] as a a potential goose laying golden eggs. Indeed, while Quantum Computing has been around since Benioff [1], Deutsch [7], Feynman [8] and Manin [12] suggested that a quantum computer could perform tasks out of reach for classical computers, it really started getting some traction when Shor [17] unearthed a polynomial-time quantum algorithm to factor integers. Since then, huge efforts have been made to actually build quantum hardware; only recently though have researchers, in a partnership between Google AI and the US NASA, managed to stabilise a quantum chip over a short period of time, effectively starting what has already been called the Quantum Revolution. Several companies are now proposing online quantum capabilities, using a few qubits. We are still far from being able to use those in production mode on a large scale, but the revolution is fast marching, and tools are urgently needed to embrace it. Quantitative Finance is traditionally quick to respond to such calls, and several attempts have recently been made to use quantum techniques for option pricing, in particular [16, 18], focusing on the so-called Amplitude Estimation algorithm [4], which allows a quadratic speed-up for simulation methods compared to classical Monte Carlo schemes.

We propose a new route to investigate the use of Quantum techniques in Quantitative Finance, and develop a hybrid quantum-classical algorithm to solve the Schrödinger equation, which by simple transformations is equivalent to the PDE satisfied by the option price. The paper is organised as follows. In Section 2, we introduce the main tools and notations, clarifying the link between the Black-Scholes PDE [3] and its Schrödinger counterpart along the imaginary axis, while providing a short reminder on Quantum mechanics. In Section 3, we borrow an idea developed in quantum chemistry [10], and propose an algorithm to solve the aforementioned Schrödinger equation using a quantum computer. The methodology develops a hybrid algorithm, where part of the computations can be run on a quantum computer, while the remaining tasks are solved on a classical machine. We describe in detail in Section 4 the actual implementation of the algorithm,

Date: December 5, 2019.

2010 *Mathematics Subject Classification.* 35Q40, 91G20, 91G80.

Key words and phrases. quantum algorithms, option pricing, PDE, Schrödinger equation.

The views and opinions expressed here are the authors' and do not represent the opinions of their employers. They are not responsible for any use that may be made of these contents. No part of this presentation is intended to influence investment decisions or promote any product or service. The authors would like to thank Alexei Kondratyev for stimulating discussions.

with a particular emphasis on the quantum circuit. The numerical results are presented in Section 5, and we show that the shallow quantum circuit developed here is able to price European and arithmetic Asian options in the Black-Scholes model with very good accuracy.

2. Black-Scholes and the Schrödinger equation

The Black-Scholes model is at the core of financial modelling and assumes that, under a given risk-neutral measure, the underlying stock price process $(S_t)_{t\geq 0}$ satisfies the stochastic differential equation

$$\frac{\mathrm{d}S_t}{S_t} = r\mathrm{d}t + \sigma \mathrm{d}W_t, \qquad \text{for } t \geq 0, \tag{2.1}$$

where W is a standard Brownian motion on a given filtered probability space, $r \in \mathbb{R}$ is the instantaneous risk-free rate, and $\sigma > 0$ is the instantaneous volatility. There is a vast literature extending this model in many different directions and using a plethora of numerical techniques, ranging from PDEs to Monte Carlo and Fourier methods. We are here chiefly interested in developing a quantum-based algorithm for PDEs, and will hence ignore numerical methods apart from the PDE approach, considering only European financial derivatives, with no early exercise.

2.1. Pricing PDEs.

For a European Call option with payoff $f(S_T) = \max(S_T - K, 0)$ at maturity T, the Feynman-Kac formulation allows us to write the option price $V(t,s) := \mathbb{E}\left[\mathrm{e}^{-r(T-t)} f(S_{(T)}) | S_t = s\right]$, for any $t \in [0,T]$, obtained by no-arbitrage arguments, as the unique smooth solution to the PDE

$$\left(\partial_t + \frac{\sigma^2 s^2}{2}\partial_{ss} + rS\partial_s - r\right) V(t,s) = 0, \tag{2.2}$$

for all $s > 0$, $t \in [0,T)$, with terminal condition $V(T,s) = f(s)$. The changes of variables $S = \mathrm{e}^x$ and $\tau = \sigma^2(T-t)$ reduce this partial differential equation to the heat equation

$$\partial_\tau u(\tau, x) = \frac{1}{2}\partial_{xx} u(\tau, x), \tag{2.3}$$

on $(0, \sigma^2 T] \times \mathbb{R}$, with boundary condition $u(0,x) = \mathrm{e}^{-ax} f(\mathrm{e}^x)$, where $b := \frac{1}{4\sigma^2}\left(\frac{1}{2} - \frac{4r}{2\sigma^2} - \sigma^2 - 2r\right)$ and $a := \frac{1}{2} - \frac{r}{\sigma^2}$. Another common financial derivative is the fixed-strike arithmetic Asian Call option, with terminal payoff

$$\max\left(\frac{1}{T}\int_0^T S(t)\mathrm{d}t - K, 0\right), \tag{2.4}$$

for some strike $K > 0$. Setting $Y_t := \left(B_t - K\mathrm{e}^{-r(T-t)}\right)/S_t$ with

$$B_t = q(t)S_t + \frac{\mathrm{e}^{-r(T-t)}}{T}\int_0^t S_u \mathrm{d}u \qquad \text{and} \qquad q(t) = \begin{cases} \dfrac{1 - \mathrm{e}^{-r(T-t)}}{rT}, & \text{if } r \neq 0, \\ 1 - \dfrac{t}{T}, & \text{if } r = 0, \end{cases}$$

Brown [5] and Vecer [19] showed that the price at time $t \in [0,T)$ of the option reads $V(t,S_t) = S_t \widetilde{Q}(t, Y_t)$. With $\tau := \sigma^2(T-t)$ and $Q(\tau, y) = \widetilde{Q}(t,y)$, the function Q uniquely solves the PDE

$$\partial_\tau Q(\tau, y) = \frac{(q(\tau) - y)^2}{2}\partial_{yy} Q(\tau, y), \tag{2.5}$$

for $(\tau, y) \in (0, \sigma^2 T] \times \mathbb{R}$ with terminal condition $Q(0,y) = \max(y, 0)$, while the space boundaries are set as $\lim_{y \downarrow -\infty} Q(\tau, y) = 0$ and $Q(\tau, q(0)) = q(0)$. One should note that (2.5) is very similar to the heat equation (2.3), albeit with an additional time-dependence on the right-hand side.

2.2. **Schrödinger's formulation.** We now translate the two pricing PDEs (2.3) and (2.5) into a linear Schrödinger equation, classical in quantum mechanics. The Wick rotation $\xi = -\mathrm{i}\tau$, where i is the imaginary unit, transforms (2.3) into

$$-\mathrm{i}\partial_\xi u(\xi, x) = \frac{1}{2}\partial_{xx} u(\xi, x),$$

which, in the quantum computing literature, is often written using Dirac's notation (see Section 2.3) as

$$-\mathrm{i}\frac{\partial}{\partial\xi}\left|\psi\right\rangle = \widehat{\mathcal{H}}\left|\psi\right\rangle, \tag{2.6}$$

where the wave function ψ (and its associated quantum state $|\psi\rangle$) plays the role of the modified derivative price $u(\cdot,\cdot)$, while the Hamiltonian operator is simply $\widehat{\mathcal{H}} = \frac{1}{2}\partial_{xx}$. For this special case of a time-independent Hamiltonian, the solution to (2.6) is given explicitly by

$$\left|\psi(\xi)\right\rangle = \exp\left(\mathrm{i}\widehat{\mathcal{H}}\xi\right)\left|\psi(0)\right\rangle, \tag{2.7}$$

where $\exp\left(\mathrm{i}\widehat{\mathcal{H}}\xi\right)$ is the time evolution operator, and $|\psi(0)\rangle$ a normalised initial state with $\langle\psi(0)|\psi(0)\rangle = 1$. For Asian options, the Wick rotation $\xi = -\mathrm{i}\tau$ now turns (2.5) into

$$-\mathrm{i}\partial_\xi Q(\tau, y) = \frac{\left(q(\tau) - Y\right)^2}{2}\partial_{yy} Q(\tau, y),$$

which reads, in Dirac's notations,

$$-\mathrm{i}\frac{\partial}{\partial\xi}\left|\psi\right\rangle = \widehat{\mathcal{H}}(\xi)\left|\psi\right\rangle. \tag{2.8}$$

The main difference between (2.6) and (2.8) is the time-dependent Hamiltonian. Nonetheless, the solution can be written by computing the new evolution operator as

$$\left|\psi(\xi)\right\rangle = \exp\left(\mathrm{i}\int_0^\xi \widehat{\mathcal{H}}(\chi)\mathrm{d}\chi\right)\left|\psi(0)\right\rangle. \tag{2.9}$$

2.3. **Reminder on quantum notations.** In order to facilitate the integration of Quantum Mechanics tools into the realm of Quantitative Finance, we shall endeavour to combine notations from both fields in a clear and consistent manner. To do so, we recall some standard Quantum notations, originating from Dirac, which we will use throughout the paper. In a given (complex-valued) Hilbert space $\mathfrak{H}$, a vector v is represented via the ket notation $|\mathrm{v}\rangle \in \mathfrak{H}$. For $\mathrm{u} \in \mathfrak{H}$, the bra $\langle\mathrm{u}|$ belongs to the dual space $\mathfrak{H}^*$, so is a linear map from $\mathfrak{H}$ to $\mathbb{C}$, and we denote the action of u on v as the bracket $\langle\mathrm{u}|\mathrm{v}\rangle$. In classical linear algebra notations, this can be recast in the following form: suppose that $\mathfrak{H}$ is of dimension $n \in \mathbb{N}$, then $\mathrm{u}, \mathrm{v} \in \mathfrak{H}$ can be represented as vectors in $\mathbb{R}^n$ as

$$\mathrm{u} = \begin{pmatrix} u_1 \\ \vdots \\ u_n \end{pmatrix} \qquad \text{and} \qquad \mathrm{v} = \begin{pmatrix} v_1 \\ \vdots \\ v_n \end{pmatrix},$$

or $\mathrm{u} = (u_1, \ldots, u_n)^\top$ and $\mathrm{v} = (v_1, \ldots, v_n)^\top$. In that case, we can write

$$|\mathrm{v}\rangle = \begin{pmatrix} v_1 \\ \vdots \\ v_n \end{pmatrix}, \qquad \langle\mathrm{u}| = (u_1^*, \ldots, u_n^*), \qquad \text{and} \qquad \langle\mathrm{u}|\mathrm{v}\rangle = \sum_{i=1}^n u_i^* v_i,$$

where * denotes complex conjugacy. A physical state in quantum mechanics is represented by a state vector, or in fact a ket. The general quantum state of a qubit, the basic unit of quantum information, is a linear superposition of its orthonormal basis. In particular, a single qubit state can be written as $|\psi\rangle = \alpha\left|0\right\rangle + \beta\left|1\right\rangle$, for some $\alpha, \beta \in \mathbb{C}$ satisfying $|\alpha|^2 + |\beta|^2 = 1$, with $(|0\rangle, |1\rangle)$ the orthonormal basis. In classical linear algebra notations, this boils down to

$$\psi = \begin{pmatrix} \psi_1 \\ \psi_2 \end{pmatrix} = \alpha\begin{pmatrix} 1 \\ 0 \end{pmatrix} + \beta\begin{pmatrix} 0 \\ 1 \end{pmatrix}.$$

Generally speaking, an n-qubit quantum state corresponds to a vector in $\mathbb{C}^{2^n}$. For such a state $|\psi\rangle$, that is, a physical system which can be in n different, mutually exclusive classical states $|0\rangle, |1\rangle, \dots, |n-1\rangle$, so that

$$|\psi\rangle = \alpha_0 |0\rangle + \cdots + \alpha_{n-1} |n-1\rangle,$$

for $(\alpha_0, \dots, \alpha_{n-1}) \in \mathbb{C}^n$, such that $\sum_{i=1}^n |\alpha_i|^2 = 1$. The basis $(|0\rangle, |1\rangle, \dots, |n-1\rangle)$ forms an orthonormal basis of an n-dimensional Hilbert space $\mathfrak{H}_n$. Given $\mathfrak{H}_n$ and $\mathfrak{H}_m$, we can define the tensor product $\mathfrak{H} := \mathfrak{H}_n \otimes \mathfrak{H}_m$ as the nm-dimensional Hilbert space spanned by $\{|i\rangle \otimes |j\rangle : i = 0, \dots, n-1, j = 0, \dots, m-1\}$. For example, a 2-qubit system, corresponding to a Hilbert space of dimension 4 can be viewed as the tensor product of two Hilbert spaces, each of dimension 2, and its basis being spanned by $\{|0\rangle \otimes |0\rangle, |0\rangle \otimes |1\rangle, |1\rangle \otimes |0\rangle, |1\rangle \otimes |1\rangle\}$, which can also be written as $\{|00\rangle, |01\rangle, |10\rangle, |11\rangle\}$.

Quantum logic gates are reversible quantum circuits operating on quantum states, which can be represented as unitary matrices. We shall here make use of several particular gates repeatedly, which can be easily represented in a 1-qubit state as the following 2×2 matrices:

$$\begin{array}{lll} \mathbf{X}: & \text{X-Pauli gate:} & \begin{pmatrix} 0 & 1 \\ 1 & 0 \end{pmatrix} \\ \mathbf{Y}: & \text{Y-Pauli gate:} & \begin{pmatrix} 0 & -\mathrm{i} \\ \mathrm{i} & 0 \end{pmatrix} \\ \mathbf{H}: & \text{Hadamard gate:} & \frac{1}{\sqrt{2}} \begin{pmatrix} 1 & 1 \\ 1 & -1 \end{pmatrix} \\ \mathbf{R}_y(\theta): & \text{Rotation gate with angle } \theta: & \begin{pmatrix} \cos\left(\frac{\theta}{2}\right) & -\sin\left(\frac{\theta}{2}\right) \\ \sin\left(\frac{\theta}{2}\right) & \cos\left(\frac{\theta}{2}\right) \end{pmatrix} \end{array} \tag{2.10}$$

3. Quantum Imaginary Time Evolution

We now describe a strategy to solve the linear Schrödinger equation along its imaginary time axis using a quantum computer. Our approach relies on the hybrid algorithm developed in [10], where part of the computation is performed on a quantum computer, and part on a classical machine. Consider first a time-independent Hamiltonian $\widehat{\mathcal{H}}$ with evolution operator (or propagator) $\exp(\mathrm{i}\widehat{\mathcal{H}}\xi)$ evolving along real values ξ. In this case, the propagator can be implemented efficiently on a quantum computer by means of a Trotter decomposition, since $\exp(\mathrm{i}\widehat{\mathcal{H}}\xi)$ is a unitary matrix [14]. Along the imaginary axis however, the corresponding evolution operator $\exp(\widehat{\mathcal{H}}\tau)$ is represented by a non-unitary matrix; It can be easily simulated on a classical computer, however as the dimension of the wave function grows exponentially, it rapidly becomes infeasible; its Trotter decomposition using unitary gates is not straightforward, making its implementation on a quantum computer more challenging. We follow instead a recent idea [10] to solve an equivalent normalised imaginary time evolution

$$|\psi(\tau)\rangle = \gamma(\tau)\, \mathrm{e}^{\widehat{\mathcal{H}}\tau} |\psi(0)\rangle, \qquad \text{with } \gamma(\tau) := \left(\langle\psi(0)| \, \mathrm{e}^{2\widehat{\mathcal{H}}\tau} |\psi(0)\rangle\right)^{-1/2}, \tag{3.1}$$

indirectly. The parameter $\gamma(\tau)$ is a normalisation constant, and $\widehat{\mathcal{H}}$ a time-independent Hamiltonian. We call this approach indirect since $|\psi(\tau)\rangle$ is not computed by constructing the operator $\exp(\widehat{\mathcal{H}}\tau)$ on a quantum computer. Instead, we approximate $|\psi(\tau)\rangle$ by a quantum circuit composed of a sequence of parameterised gates such that $|\psi(\tau)\rangle \approx |\phi(\boldsymbol{\theta}_\tau)\rangle$, where $\boldsymbol{\theta}_\tau = (\theta_\tau^1, \cdots, \theta_\tau^N)^\top \in \mathbb{R}^N$ is a vector of time-dependent parameters. Therefore, knowing how to describe the evolution of $\boldsymbol{\theta}_\tau$ makes it possible to reconstruct the imaginary Schrödinger time evolution $|\psi(\tau)\rangle$ in (3.1). We shall refer to the approximation $|\phi(\boldsymbol{\theta}_\tau)\rangle$ as the ansatz circuit.

Assume that our initial quantum state is $|\psi_{\text{init}}\rangle$, so that the ansatz at time τ_0 is $|\phi(\boldsymbol{\theta}_{\tau_0})\rangle = \Phi(\boldsymbol{\theta}_{\tau_0}) |\psi_{\text{init}}\rangle$, where $\Phi(\boldsymbol{\theta}_{\tau_0})$ is sequence of unitary gates $\Phi(\boldsymbol{\theta}_{\tau_0}) = \mathcal{S}\left(\mathrm{U}_N(\theta_{\tau_0}^N), \dots, \mathrm{U}_k(\theta_{\tau_0}^k), \dots, \mathrm{U}_1(\theta_{\tau_0}^1)\right)$ which we will specify later. In this paper, each parameterised gate $\mathrm{U}_k(\theta^k)$ is considered as a rotation or a controlled rotation gate. It is also possible to show that the evolution of $\boldsymbol{\theta}_\tau$, and thus the Schrödinger imaginary time dynamics, can be computed using McLachlan's variational principle [11]

$$\delta \left\| \left(\partial_\tau + \widehat{\mathcal{H}}\right) |\psi(\tau)\rangle \right\| = 0, \tag{3.2}$$

where $\|v\| := \langle v|v\rangle$, and δ denotes the infinitesimal variation. This determines the values of $\boldsymbol{\theta}_\tau$ minimising the distance $\| \, |\psi(\tau)\rangle - |\phi(\boldsymbol{\theta}_\tau)\rangle \, \|$. The variational principle (3.2) results in the system of first-order ODEs [10]

$$\mathrm{A}(\tau)\dot{\boldsymbol{\theta}}_\tau = \mathrm{C}_\tau, \qquad \text{for each } \tau, \tag{3.3}$$

where $\dot{\boldsymbol{\theta}}\tau = \partial_\tau \boldsymbol{\theta}_\tau$, and the matrix $\mathrm{A}(\tau)$ and the vector $\mathrm{C}(\tau)$ read

$$\mathrm{A}(\tau) = \left(\Re\left(\frac{\partial \langle \phi(\tau)|}{\partial \theta^i} \frac{\partial |\phi(\tau)\rangle}{\partial \theta^j} \right) \right)_{i,j=1,\dots,N} \qquad \text{and} \qquad \mathrm{C}(\tau) = \left(\Re\left(\frac{\partial \langle \phi(\tau)|}{\partial \theta^i} \widehat{\mathcal{H}} |\phi(\tau)\rangle \right) \right)_{i=1,\dots,N}.$$

One of the main advantages of this method is that both A and C can be measured efficiently using a quantum computer [2, 10]. In order to build the hybrid classical-quantum scheme, we rely on the following assumptions:

Assumption 3.1.

(i) Every unitary gate in the algorithm depends on a single parameter.
(ii) The decomposition

$$\widehat{\mathcal{H}} = \sum_{i=1}^{N} \lambda_i h_i$$

holds, where λ_i are real coefficients and h_i are tensor products of Pauli matrices.

Assumption 3.1(i) is in fact purely for convenience, as unitary gates with multiple parameters can be easily decomposed into single-parameter ones. It in particular allows us to write, for every $k = 1 \dots, N$, the derivative of the unitary gate U_k as

$$\partial_{\theta^k} \mathrm{U}_k(\theta^k) = \sum_{i=1}^{N} f_{k,i} \mathrm{U}_k(\theta^k) \sigma_{k,i},$$

where $\sigma_{k,i}$ is a single-qubit or a two-qubit unitary operator, while $f_{k,i}$ is a scalar parameter, which in turn implies

$$\partial_{\theta^k} |\phi(\tau)\rangle = \sum_{i=1}^{N} f_{k,i} \widetilde{\Phi}_{k,i} |\psi_{\text{init}}\rangle, \qquad \text{where} \qquad \widetilde{\Phi}_{k,i} = \mathcal{S}\left(\mathrm{U}_N(\theta^N), \dots, \mathrm{U}_k(\theta^k)\sigma_{k,i}, \dots, \mathrm{U}_1(\theta^1) \right).$$

For example, if $\mathrm{U}_k(\theta^k)$ is a single-qubit $\mathbf{R}_y(\theta^k)$ rotation gate such that $\mathrm{U}_k(\theta^k) = \exp\left(-\frac{1}{2}\mathrm{i}\theta^k \sigma_Y\right)$, where σ_Y is the Y-Pauli matrix, the derivative is simply $\partial_{\theta^k} \mathrm{U}_k(\theta^k) = -\frac{\mathrm{i}\sigma_Y}{2} \mathrm{U}_k(\theta^k)$. Therefore, the state $\partial_{\theta^k} |\phi(\tau)\rangle$ can be prepared by adding the extra σ_Y gate, together with a constant factor $-\frac{\mathrm{i}}{2}$ only, such that $\partial_{\theta^k} |\phi(\tau)\rangle = -\frac{\mathrm{i}}{2} \widetilde{\Phi}_{k,k}(\boldsymbol{\theta}) |\psi_{\text{init}}\rangle$, where $\widetilde{\Phi}_{k,k}(\boldsymbol{\theta}) = \mathcal{S}(\mathrm{U}_N(\theta^N), \dots, \mathrm{U}_k(\theta^k)\sigma_Y, \cdots, \mathrm{U}_1(\theta^1))$. In general, the matrix A is then computed as [10]

$$\mathrm{A}_{ij} = \Re\left(\sum_{k,l=1,\dots,N} f^*_{k,i} f_{l,j} \langle \psi_{\text{init}}| \widetilde{\Phi}^\dagger_{k,i} \widetilde{\Phi}_{l,j} |\psi_{\text{init}}\rangle \right), \qquad \text{for } i,j = 1, \dots, N, \tag{3.4}$$

where the dagger † denotes the complex conjugate of the transpose. Moreover, an equivalent circuit designed to measure the matrix A using a quantum computer, directly, is discussed in [2, 10]. We will also present an example of a quantum circuit to measure an element of A in Section 4.

For the vector C, we use Assumption 3.1(ii); however, this decomposition usually scales polynomially with the system size, since $\widehat{\mathcal{H}}$ is a sparse matrix obtained from the discretisation of a differential operator. The corresponding vector C then reads [10]

$$\mathrm{C}_i = \Re\left(\sum_{k,j=1,\dots,N} f^*_{k,i} \lambda_j \langle \psi_{\text{init}}| \widetilde{\Phi}^\dagger_{k,i} h_j \Phi |\psi_{\text{init}}\rangle \right), \qquad \text{for } i = 1, \dots, N.$$

Once the matrix A and the vector C are obtained, the time evolution can be computed numerically using a classical computer. We suggest here an Euler scheme, as in [10], and the evolution of $\boldsymbol{\theta}_{\tau+\Delta_\tau}$ is calculated as

$$\boldsymbol{\theta}_{\tau+\Delta_\tau} = \boldsymbol{\theta}_\tau + \Delta_\tau \dot{\boldsymbol{\theta}}_\tau = \boldsymbol{\theta}_\tau + \Delta_\tau \mathrm{A}(\tau)^{-1} \mathrm{C}(\tau), \tag{3.5}$$

for some small time step Δ_τ. Usually, the matrix A is not well-conditioned, and we solve, for each τ

$$\arg\min \left\{ \left\| \mathrm{A}(\tau)\dot{\boldsymbol{\theta}}_\tau - \mathrm{C}(\tau) \right\| : \boldsymbol{\theta}_\tau \in \mathbb{R}^N \right\}, \tag{3.6}$$

instead of (3.3) directly, assuming some small cut-off ratio[1] for the eigenvalues of A.

[1]This computation is straightforward in `Python` using the package `numpy.linalg.lstsq` for example.

For a time-dependent Hamiltonian, for Asian options, we are interested in determining the quantum state

$$|\psi(\tau)\rangle = \gamma(\tau)\ \exp\left(\int_0^\tau \widehat{\mathcal{H}}(\chi)\mathrm{d}\chi\right)|\psi(0)\rangle\,, \quad \text{with } \gamma(\tau) := \left(\langle\psi(0)|\exp\left\{2\int_0^\tau \widehat{\mathcal{H}}(\chi)\mathrm{d}\chi\right\}|\psi(0)\rangle\right)^{-\frac{1}{2}} \tag{3.7}$$

instead of (3.1), with the new normalisation constant. In order to avoid the integral calculation in (3.7), we use, along a left-point approximation when discretising of the integral, effectively freezing the time-dependent Hamiltonian $\widehat{\mathcal{H}}(\tau)$ on every time interval; thus the only difference with the time-independent framework above is the update of the Hamiltonian at every time step. The main drawback of the present approach is the requirement for an ansatz circuit. Ideally, the latter has to be complex enough to approximate the underlying quantum state $|\psi(\tau)\rangle$, but not unnecessarily deep in order to avoid the expensive computation (on a classical computer) of the linear problem (3.6), i.e. too many parameters $\boldsymbol{\theta}$. In the examples below, we design a quantum circuit strategy for simple financial derivatives, and obtain promising results for relatively shallow quantum circuits.

4. Hybrid Quantum-Classical Algorithm

We now design the quantum imaginary time algorithm described in Section 3 to price financial derivatives. The main challenge is to design an ansatz circuit able to represent the price of the underlying option from expiry down to the valuation date. We here employ the sequence of gates described by the quantum circuit depicted in Figure 1.

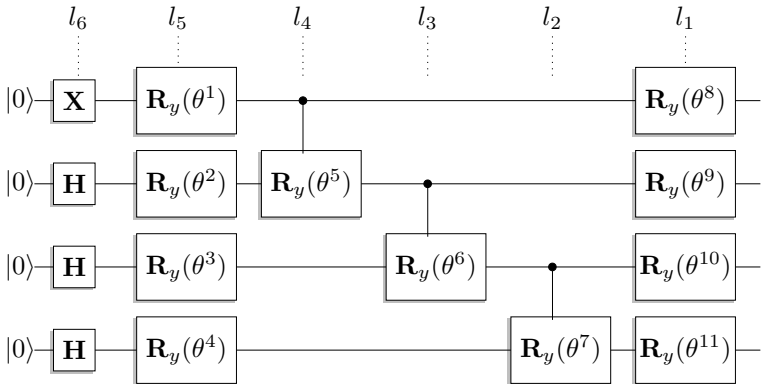

Figure 1. Ansatz implemented for European and Asian Call options. The vector $\boldsymbol{\theta}$ is composed by the angles of each rotation gate. The notations $l_1, \ldots, l_6$ indicate the different layers.

Remark 4.1. In Figure 1, a line represents a qubit, whereas a squared box denotes the action of a quantum gate on the qubit on this line. The circuit is to be read from left (inputs) to right (outputs). A controlled gate (for example $\mathbf{R}(\theta^5)$) is shown with a filled black circle on the control qubit line, and the usual symbol for the gate is written on the target qubit, with a line connecting the two.

The quantum circuit has 4 qubits only, and thus our strategy is able to recover Call prices with a resolution of $2^4 = 16$ points. The ansatz in Figure 1 has a layer l_6 composed by $\mathbf{H}$ and $\mathbf{X}$ gates (2.10). In the next layer l_5, a sequence of $\mathbf{R}_y$ gates is applied to each qubit. Each such gate has a free parameter that needs to be calculated given some desired initial condition, and these parameters vary in time, as described above. The layers l_4, l_3 and l_2, composed by controlled $\mathbf{R}_y^c$ gates, and a new layer l_1, similar to l_5, are added in order to give more flexibility to the approximation, and thus achieve different and more involved values of $|\phi(\boldsymbol{\theta}_\tau)\rangle$. In the present analysis, we increase or reduce the complexity of the ansatz circuit by adding or removing new unit cells, i.e. layers l_4, l_3, l_2 and l_1. The optimal configuration is obtained when $|\phi(\boldsymbol{\theta}_0\rangle$ is able to represent $|\psi(0)\rangle$ with good accuracy, and with as few free parameters as possible. One should note that the ansatz is composed of gates with rotations along the y axis only. The motivation for using $\mathbf{R}_y$ gates is due to its real-valued representation, which is desirable as $|\psi(\tau)\rangle$ in (3.1) is a real number. However, other approaches might also be valid, using for instance $\mathbf{R}_x$ and $\mathbf{R}_z$ gates, at the cost of computing the real part of $|\phi(\boldsymbol{\theta}_\tau)\rangle$ at the end of the simulations.

Mathematically, a quantum circuit is described by means of a series of matrix operations; the ansatz in Figure 1 is composed of $\mathbf{X}$, $\mathbf{H}$, and $\mathbf{R}_y$ single-qubits gates, and their mathematical representations are given by the matrices in (2.10). The controlled rotation gate $\mathbf{R}_y^c$ is implemented using two qubits, and its matrix representation reads

$$\mathbf{R}_y^c(\theta) := \begin{pmatrix} 1 & 0 & 0 & 0 \\ 0 & 1 & 0 & 0 \\ 0 & 0 & \cos\left(\frac{\theta}{2}\right) & -\sin\left(\frac{\theta}{2}\right) \\ 0 & 0 & \sin\left(\frac{\theta}{2}\right) & \cos\left(\frac{\theta}{2}\right) \end{pmatrix} = \begin{pmatrix} \mathbf{I}_2 & \mathbf{O}_2 \\ \mathbf{O}_2 & \mathbf{R}_y(\theta) \end{pmatrix},$$

where $\mathbf{O}_2$ denotes the 2×2 null matrix. The resulting mathematical representation of the quantum circuit in Figure 1 is calculated by grouping all quantum gates accordingly. For example, the effect of the layer l_1 in Figure 1, which contains the gates $\mathbf{R}_y(\theta^8)$, $\mathbf{R}_y(\theta^9)$, $\mathbf{R}_y(\theta^{10})$ and $\mathbf{R}_y(\theta^{11})$, is computed as

$$\boldsymbol{\mathcal{E}}^{l_1} = \mathbf{R}_y(\theta^8) \otimes \mathbf{R}_y(\theta^9) \otimes \mathbf{R}_y(\theta^{10}) \otimes \mathbf{R}_y(\theta^{11}),$$

where $\otimes$ represents the Kronecker product. The effect of $\mathbf{R}_y^c(\theta^7)$ in l_2 is calculated similarly as

$$\boldsymbol{\mathcal{E}}^{l_2} = \mathbf{I}_2 \otimes \mathbf{I}_2 \otimes \mathbf{R}_y^c(\theta^7),$$

with $\mathbf{I}_2$ the 2×2 identity matrix, and the combined effect of $\boldsymbol{\mathcal{E}}^{l_1}$ and $\boldsymbol{\mathcal{E}}^{l_2}$ is the standard matrix multiplication

$$\boldsymbol{\mathcal{E}}^{l_1,l_2} = \boldsymbol{\mathcal{E}}^{l_1} \times \boldsymbol{\mathcal{E}}^{l_2}.$$

This process is then repeated until the whole quantum circuit is completed, and the resulting effect of the six layers in Figure 1 reads

$$\boldsymbol{\mathcal{E}}^{l_1,\ldots,l_6} = \prod_{i=1}^{6} \boldsymbol{\mathcal{E}}^{l_i}.$$

With this circuit, the final output $|\psi_{\mathrm{F}}\rangle$ of the quantum circuit due to the input $|\psi_{\mathrm{init}}\rangle$ is then computed as

$$|\psi_{\mathrm{F}}\rangle = \boldsymbol{\mathcal{E}}^{l_1,\ldots,l_6} |\psi_{\mathrm{init}}\rangle .$$

For example, the input $|\psi_{\mathrm{init}}\rangle$ of the ansatz circuit in Figure 1 is a quantum state where each of the 4 qubits is $|0\rangle$. Its vectorial representation is thus

$$|\psi_{\mathrm{init}}\rangle = |0\rangle \otimes |0\rangle \otimes |0\rangle \otimes |0\rangle$$

Finally, note that if $\boldsymbol{\theta} = 0$, the resulting state $|\phi(\boldsymbol{\theta})\rangle$ becomes a step function, since each gate $\mathbf{R}_y$ behaves as the identity operator $\mathbf{I}_2$. As discussed above, the payoff of each financial product needs to be represented by the ansatz $|\phi(\boldsymbol{\theta}_0)\rangle$ before starting the actual simulation. In practice, this representation is implemented by computing the values of $\boldsymbol{\theta}_0$ which best describes the initial conditions of the algorithm, that is

$$\boldsymbol{\theta}_0 = \underset{\boldsymbol{\theta} \in \mathbb{R}^N}{\arg\min} \left\{ \| |\phi(\boldsymbol{\theta})\rangle - |\psi(0)\rangle \| \right\}. \tag{4.1}$$

The quantum state $|\psi(0)\rangle$ is calculated directly from the payoff $f(\cdot)$ of each financial derivative. In the case of an European option, the state $|\psi(0)\rangle$ is simply $|\psi(0)\rangle \equiv \gamma(0)\mathrm{e}^{-aX} f(\mathrm{e}^X)$, where $\gamma(0)$ is the normalisation constant guaranteeing $\langle\psi(0)|\psi(0)\rangle = 1$, and a comes from the change of variables from the Black-Scholes PDE to the heat equation in (2.3). Some care should be taken when solving (4.1) since the cost function is not convex, and algorithms such as Differential Evolution will avoid being trapped in a local minimum. Ideally, the design of the ansatz should be considered together with the optimisation problem (4.1). In practice, if the ansatz circuit is not able to represent the payoff $|\psi(0)\rangle$ accurately, it becomes pointless to compute the time-marching simulation $|\phi(\boldsymbol{\theta}_\tau)\rangle$ since the algorithm already starts from the wrong initial conditions. In this case, the quantum circuit in Figure 1 needs to be improved for the desired application. The complete strategy to define the depth of the ansatz in Figure 1 and its initial condition $\boldsymbol{\theta}_0$ is summarised in Table 1.

Ansatz and initial condition algorithm

input ← Payoff function
initialisation:
Define the normalised initial condition $|\psi(0)\rangle$
Define the maximum acceptable number of unit cells $N_{\text{cells}}^{\max}$
Define the maximum acceptable error $\varepsilon^{\max} = \| \, |\phi(\boldsymbol{\theta}_0)\rangle - |\psi(0)\rangle \, \|$
Define an initial ansatz with N_{cells} unit cells
end
while $N_{\text{cells}} < N_{\text{cells}}^{\max}$
Compute the optimal $\boldsymbol{\theta}_0$ from (4.1) and the approximation error $\varepsilon = \| \, |\phi(\boldsymbol{\theta}_0)\rangle - |\psi(0)\rangle \, \|$
if $\varepsilon > \varepsilon^{\max}$
Increase the number of unit cells N_{cells} in the ansatz
else
output → Ansatz circuit and initial condition $\boldsymbol{\theta}_0$
end
end
output → Inform that the algorithm has not converged and that a different ansatz is needed

Table 1. Algorithm to determine the depth of the ansatz and the initial conditions $\boldsymbol{\theta}_0$.

The main advantage of the hybrid scheme is that the matrix A and the vector C in (3.3) can each be measured on a quantum computer. For example, $\mathrm{A}_{2,8}$ can be measured using the quantum circuit in Figure 2.

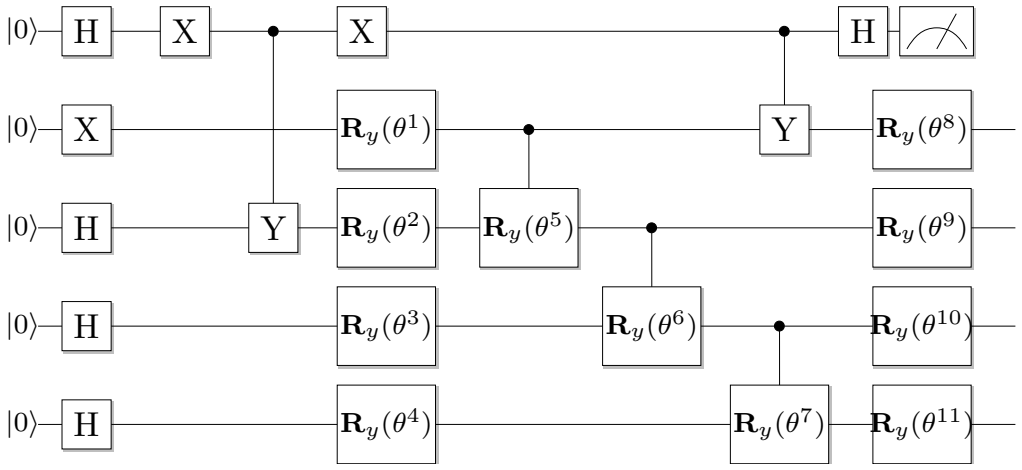

Figure 2. Quantum circuit able to measure $\mathrm{A}_{2,8}$ in (3.3). The symbol on the top right of the Figure denotes measurement of the quantum state.

In summary, we need to add an ancillary qubit to the quantum circuit of Figure 1 together with two **H** and **X** gates, and a controlled $\mathbf{R}_y^c$ gate before each respective gate $\mathbf{R}_y(\theta^2)$ and $\mathbf{R}_y(\theta^8)$. In the following, $\mathrm{A}_{2,8}$ is obtained by measuring the expectation value on the added ancillary qubit, as in [2, 10]. The determination of C is implemented on a quantum computer using a very similar approach. The main difference is that the underlying Hamiltonian $\widehat{\mathcal{H}}$ first needs to be decomposed according to Assumption 3.1(ii). Table 2 below summarises the structure of the hybrid quantum-classical algorithm, where the labels (CC) and (QC) indicate which part of the algorithm should be computed on a classical and on a quantum computer respectively.

Remark 4.2. The current methodology only checks the quantum approximation accuracy at the payoff level, i.e. verifying $\| \, |\phi(\boldsymbol{\theta}_0)\rangle - |\psi(0))\rangle \, \| = \mathcal{O}(\varepsilon)$, for some tolerance level ε, assuming that the error does not propagate much along the grid, namely that $\| \, |\phi(\boldsymbol{\theta}_\tau)\rangle - |\psi(\tau))\rangle \, \|$ remains of order ε for all τ. This assumption may fail in cases where the price $|\psi(\tau)\rangle$ varies significantly. One computational issue of the scheme is the resolution of the high-dimensional minimisation problem (4.1). Other imaginary-time evolution

Hybrid quantum-classical algorithm	
input ← Ansatz circuit and initial condition $\boldsymbol{\theta}_0$	
initialisation:	
Define the initial condition for the ansatz, i.e. $\lvert\phi(\boldsymbol{\theta}_0)\rangle$:	
Define the Hamiltonian $\widehat{\mathcal{H}}$ for the problem	
Decompose $\widehat{\mathcal{H}} = \sum_i \lambda_i h_i$	
end	
while $\tau < \sigma^2 T$*:*	
Compute the matrix A	(QC)
if $\widehat{\mathcal{H}}$ *is time-dependent:*	
Update the Hamiltonian $\widehat{\mathcal{H}}(\tau)$	
Update the decomposition $\widehat{\mathcal{H}}(\tau) = \sum_i \lambda_i h_i$	
end	
Compute the vector C	(QC)
Update the new values of $\boldsymbol{\theta}$	(CC)
end	
output → Price of the underlying derivative (in the original coordinates)	

Table 2. Hybrid quantum-classical algorithm.

algorithms [13] bypassing this optimisation might provide an efficient alternative for large-scale applications. We leave these two issues for further investigations.

5. Numerical Examples

We now employ the imaginary time evolution technique described above to compute the price of two different financial derivatives. The goal is to show that the proposed ansatz circuit in Figure 1 is able to reconstruct the complete price evolution of the underlying financial instruments accurately. The results show that good accuracy is obtained when the ansatz is composed by the layers in Figure 1. This configuration leads to a quantum circuit, fully described in Appendix A, composed of 25 $\mathbf{R}_y$ gates, resulting in $\boldsymbol{\theta}_\tau \in \mathbb{R}^{25}$ for each τ. Finally, we simulate the evolution of an European Call option in the Black-Scholes model using (2.3). The second example is that of a fixed-strike arithmetic Asian Call, which uses the same ansatz circuit but different initial conditions.

5.1. **European Call Option.** In the Black-Scholes model (2.1), we consider $\sigma = 20\%$, $S_0 = K = 100$, $T = 1$, and for simplicity zero interest rates. We discretise the state space on an equidistant grid bounded by $S_{\min} = 50$ and $S_{\max} = 150$, or $x_{\min} = \ln(S_{\min}) \approx 3.91$ and $x_{\max} = \ln(S_{\max}) \approx 5.01$. Using only 4 qubits, the discretisation allows the representation of $|\psi\rangle$ using $2^4 = 16$ points, where the states $|\psi_{\mathrm{F}}\rangle = |0000\rangle$ and $|\psi_{\mathrm{F}}\rangle = |1111\rangle$ represent the solution respectively at $x_{\min}$ and $x_{\max}$. The evolution of $|\phi(\boldsymbol{\theta}_\tau)\rangle$ from the expiry down to the initial date is computed using the approach described in Section 3. The Hamiltonian of the system can be written as $\widehat{\mathcal{H}} = \frac{1}{2}\partial_{xx}$ (Section 2.2), and we discretise it using second-order finite differences as

$$\begin{pmatrix} -b & 0 & 0 & 0 & \cdots & 0 & 0 & 0 \\ \frac{1}{2\Delta_x^2} & \frac{-1}{\Delta_x^2} & \frac{1}{2\Delta_x^2} & 0 & \cdots & 0 & 0 & 0 \\ 0 & \frac{1}{2\Delta_x^2} & \frac{-1}{\Delta_x^2} & \frac{1}{2\Delta_x^2} & \cdots & 0 & 0 & 0 \\ \vdots & \vdots & \vdots & \vdots & \ddots & \vdots & \vdots & \vdots \\ 0 & 0 & 0 & 0 & \cdots & \frac{1}{2\Delta_x^2} & \frac{-1}{\Delta_x^2} & \frac{1}{2\Delta_x^2} \\ 0 & 0 & 0 & 0 & \cdots & 0 & 0 & -b \end{pmatrix},$$

where Δ_x is the discretisation step in space, and the first and top rows of the matrix correspond to the behaviour at the boundaries $x_{\min}$ and $x_{\max}$, where b appears in the change of variables from the Black-Scholes PDE to the heat equation (2.3). Once the operator $\widehat{\mathcal{H}}$ is constructed, the evolution of $\boldsymbol{\theta}_\tau$ is obtained from the Euler scheme (3.5). We split the time domain $[0, T]$ into 500 equidistant steps, and compute the

matrix A and the vector C in (3.5) on this grid. Since the underlying linear system is ill-conditioned, we use the least squares approximation (3.6) to compute $\dot{\boldsymbol{\theta}}$ in (3.3) assuming an eigenvalue cutoff ration of 10^{-8}.

Figure 3 plots $|\phi(\boldsymbol{\theta}_\tau)\rangle$ using the ansatz circuit in Figure 1 and the difference between this and the price using a classical algorithm. The very low errors $\||\psi(\tau)\rangle - |\phi(\boldsymbol{\theta}_\tau)\rangle\|$ show that the proposed ansatz is able to reconstruct the evolution of $|\psi(\tau)\rangle$ very accurately, and is a promising step for the use of quantum technology in quantitative finance.

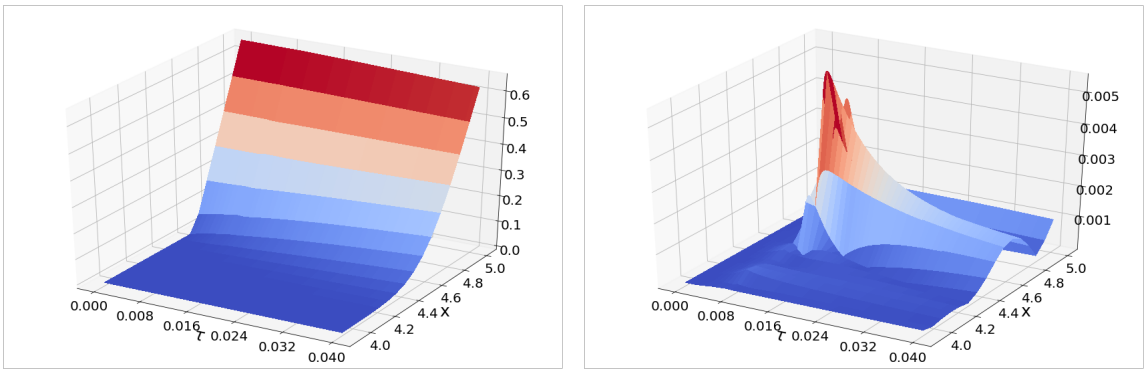

Figure 3. European Call option prices. The left plot depicts the corresponding results obtained from the quantum ansatz implementation. The right one shows the errors $\||\psi(\tau)\rangle - |\phi(\boldsymbol{\theta}_\tau)\rangle\|$.

Figure 4 compares the expected solutions to the results obtained from the simulation of the quantum algorithm. The results are depicted in the original option price coordinate system $V(t, S)$ of (2.2). The scaling parameter $\gamma(\tau)$ in (3.1) is straightforward to compute for the present case since the values of $V(t, S)$ are known at the boundary $S_{\max}$. Therefore, it is possible to determine $u(\tau, x_{\max})$ and, consequently, the scaling parameter between $|\phi(\boldsymbol{\theta}_\tau)\rangle$ and $u(\tau, x)$ in (3.1) is known. Figure 4 displays the option price at

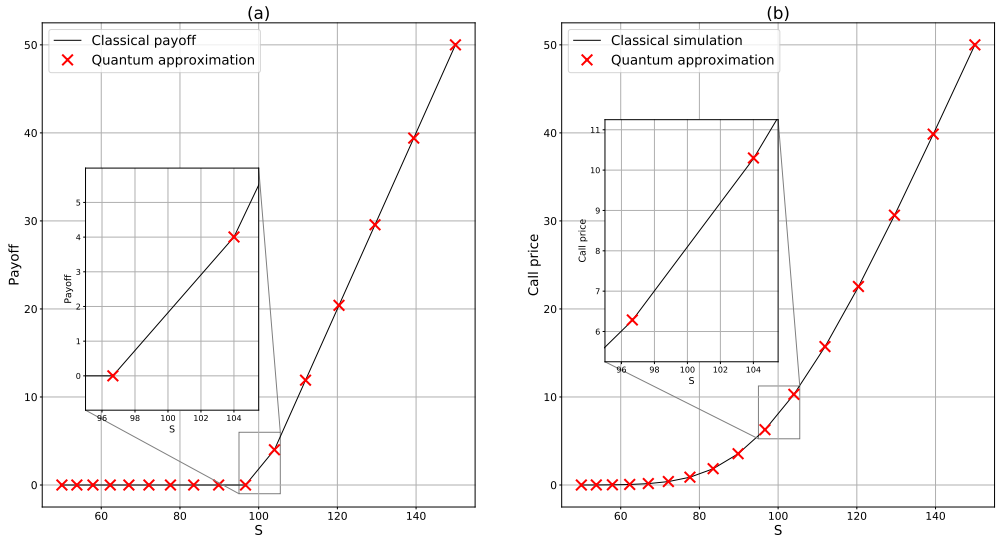

Figure 4. Prices of European Calls using the hybrid quantum-classical algorithm. The left plot shows the price at maturity and the right one at inception.

inception ($\tau = \sigma^2 T$). The hybrid quantum-classical algorithm is able to reconstruct the price function with great accuracy. We list the initial and final values of $\boldsymbol{\theta}$ in Appendix B.

5.2. **Asian Call Option.** We use the same parameters as in Section 5.1, and the same ansatz circuit in Figure 1. The system is then discretised between $y_{\min} = -0.5$ and $y_{\max} = 0.4$, corresponding to $S_{\min} \approx 66.67$ and $S_{\max} \approx 166.67$. The underlying time-dependent Hamiltonian $\widehat{\mathcal{H}}(\tau)$ is thus discretised as

$$\frac{1}{\Delta_y^2}\begin{pmatrix} 0 & 0 & 0 & \cdots & 0 & 0 & 0 \\ \frac{(q(\tau)-y_2)^2}{2} & -(q(\tau)-y_2)^2 & \frac{(q(\tau)-y_2)^2}{2} & \cdots & 0 & 0 & 0 \\ \vdots & \vdots & \vdots & \ddots & \vdots & \vdots & \vdots \\ 0 & 0 & 0 & \cdots & \frac{(q(\tau)-y_{15})^2}{2} & -(q(\tau)-y_{15})^2 & \frac{(q(\tau)-y_{15})^2}{2} \\ 0 & 0 & 0 & \cdots & 0 & 0 & 0 \end{pmatrix},$$

where $\{y_{\min}, y_2, \cdots, y_{15}, y_{\max}\}$ is the discretised space grid and Δ_y the discretisation step. The first and last rows of the matrix are null since $|\psi(\tau)\rangle$ is assumed constant at the boundaries $y_{\min}$ and $y_{\max}$. Figure 6 displays the results obtained from the classical and the quantum simulations, in the original price coordinates. Again, since the solution $Q(\tau, y)$ in (2.5) is known at the boundary $y_{\max}$, the corresponding scaling parameter linking the classical and the quantum solution is trivial to compute. Figure 6(a) depicts the payoff functions, similar to those of European Call options in Section 5.1; again, the respective errors due to the quantum approximation of the initial conditions are negligible. The results in Figure 6(b) show the option price at inception ($\tau = \sigma^2 T$). The quantum approximation obtained from the ansatz accurately match the expected values obtained by classical simulation. Finally, the initial and final values of $\boldsymbol{\theta}$ are listed in Appendix B.

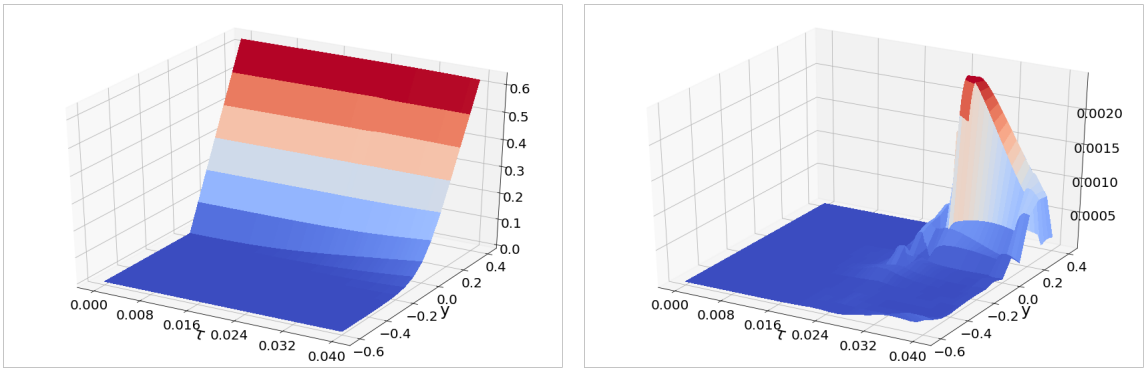

Figure 5. Asian Call option prices computed with the hybrid algorithm.

6. Conclusions and Outlook

Quantum computers are now part of the daily headlines in technology-related and financial news, and promise a new area where heavy computations can be carried out in the blink of an eye, relegating slow pricing and onerous calibration to the Middle Ages. While this promise is appealing, we are still far from it, and actual quantum computers are still in their infancy, still deeply affected by decoherence. On the software side, current quantum algorithms require a large number of qubits together with precise gate implementations, which may limit their applications in the near future. We put forward here a hybrid quantum-classical algorithm, originating in computational chemistry, to price financial derivatives. The strategy is based on the PDE representation of the pricing problem, and the link between the latter and its Schrödinger counterpart from quantum mechanics. The results show that a shallow quantum circuit is able to represent European and Asian Call option prices accurately, and therefore suggest that this approach is a promising candidate for the application of quantum computing in Finance.

The main challenge of the present methodology is the requirement for an ansatz circuit and the corresponding solution of an optimisation problem. More work is needed in the future to design an efficient ansatz for more complex financial products, or in the development of an ansatz-free approach. One of the most promising application of this technique is for basket options, based on several stocks, and hence multidimensional. Classical PDE methods suffer from the so-called curse of dimensionality, making such pricing problem cumbersome, or at least computationally intensive. Since its mathematical formulation is similar

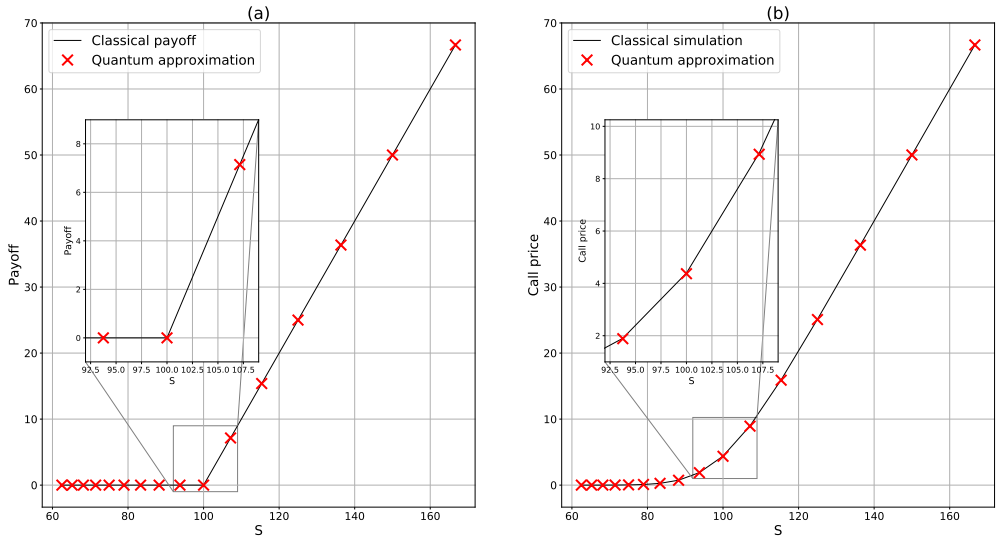

Figure 6. Arithmetic Asian Call option prices calculated using the hybrid quantum-classical algorithm. The left plot displays the expected solution and the quantum approximation for the payoff function, while the right one shows the corresponding prices at inception.

to the simulation of large-scale quantum mechanical systems governed by systems of Schrödinger equations, we believe that a modified version of our algorithm is applicable there, leveraging the power of quantum computing, and we leave this investigation for the next step.

Appendix A. Complete ansatz circuit

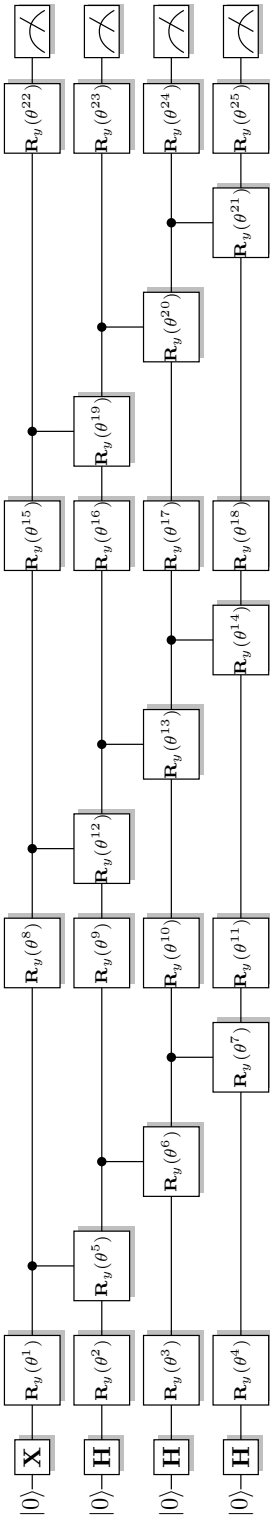

Figure 7. Ansatz circuit explained in Section 5. The circuit consists of 25 $\mathbf{R}_y$ gates.

Appendix B. Initial and terminal conditions of $\boldsymbol{\theta}$

	European Call Option		Asian Call Option	
	$\tau = 0$	$\tau = \sigma^2 T$	$\tau = 0$	$\tau = \sigma^2 T$
θ^1	3.142	3.203	3.141	3.458
θ^2	4.173	4.149	3.387	3.153
θ^3	1.392	2.278	1.282	1.108
θ^4	3.713	3.512	0.927	0.683
θ^5	2.399	2.400	4.946	4.858
θ^6	0.935	0.512	0.257	0.130
θ^7	2.196	2.578	2.937	4.062
θ^8	5.014	5.024	6.283	6.759
θ^9	2.736	2.405	4.304	3.993
θ^{10}	1.477	2.406	1.632	2.423
θ^{11}	4.472	4.271	5.103	4.859
θ^{12}	3.415	3.375	4.959	4.824
θ^{13}	6.283	6.331	4.409	3.063
θ^{14}	4.244	4.224	0.592	0.236
θ^{15}	4.711	4.347	6.283	6.599
θ^{16}	0.717	0.510	0.133	-0.693
θ^{17}	1.741	2.357	3.957	3.923
θ^{18}	1.158	0.956	0.334	0.090
θ^{19}	2.531	2.443	0.489	2.035
θ^{20}	5.705	5.232	4.940	4.582
θ^{21}	3.525	3.184	0.909	0.935
θ^{22}	4.582	4.716	3.141	3.118
θ^{23}	2.465	2.706	5.993	4.807
θ^{24}	0.098	-1.154	2.807	3.324
θ^{25}	5.018	4.817	2.783	2.539

Table 3. Values of $\boldsymbol{\theta}$ at initial and terminal times.

References

[1] P. Benioff. The computer as a physical system: a microscopic Quantum Mechanical Hamiltonian model of computers as represented by Turing machines. *Journal of Statistical Physics*, 22(563), 1980.

[2] S.C. Benjamin and Y. Li. Efficient variational quantum simulator incorporating active error minimization. *Physical Review X*, 7(2), 2017

[3] F. Black and M. Scholes. The pricing of options and corporate liabilities. *Journal of Political Economy*, 81(3): 637-654, 1973.

[4] G. Brassard, P. Hoyer, M. Mosca and A. Tapp. Quantum amplitude amplification and estimation. *AMS Contemporary Mathematics*, 305: 53-74, 2002.

[5] C. Brown, J.C. Handley, C.T. Lin and K.J. Palmer. Partial differential equations for Asian option prices. *Quantitative Finance*, 16(3), 447-460, 2016.

[6] S. Endo, I. Kurata and Y.O. Nakagawa. Calculation of the Green's function on near-term quantum computers. arXiv: 1909.12250, 2019.

[7] D. Deutsch. Quantum theory, the Church-Turing principle and the universal quantum computer. *Proceedings of the Royal Society A*, 400(1818): 97-117, 1985.

[8] R.P. Feynman. Simulating physics with computers. *International Journal of Theoretical Physics*, 21: 467-488, 1982.

[9] A. Martin, B. Candelas, A. Rodriguez-Rozas, J.D. Martin-Guerrero, X. Chen, L. Lamata, R. Orus, E. Solano and M. Sanz. Towards pricing financial derivatives with an IBM quantum computer. arXiv: 1904.05803, 2019.

[10] S. McArdle, T. Jones, S. Endo, Y. Li, S.C. Benjamin and X. Yuan. Variational ansatz based quantum simulation of imaginary time evolution. *Quantum Information*, 5(1), 2019.

[11] A. McLachlan. A variational solution of the time-dependent Schrödinger equation. *Molecular Physics*, 8(1), 39-44, 1964.

[12] Y.I. Manin. Computable and Noncomputable. *Sov.Radio*: 13-15, 1980.

[13] M. Motta, C. Sun, A. T.K. Tan, M.J. O'Rourke, E. Ye, A.J. Minnich, F. Brandao and G.K Chan. Determining eigenstates and thermal states on a quantum computer using quantum imaginary time evolution. *Nature Physics*, 2019.

[14] M.A. Nielsen and I.L. Chuang. A variational solution of the time-dependent Schrödinger equation. Cambridge University Press, 2011.

[15] R. Orus, S. Mugel and E. Lizaso. Quantum computing for finance: Overview and prospects. *Reviews in Physics*, 4, 2019.

[16] P. Rebentrost, B. Gupt and T.R. Bromley. Quantum computational finance: Monte Carlo pricing of financial derivatives. *Physical Review A*, 98(2), 2018.

[17] P.W. Shor. Algorithms for quantum computation: discrete logarithms and factoring. *Proceedings 35th Annual Symposium on Foundations of Computer Science*, 1994.

[18] N. Stamatopoulos, D.J. Egger, Y. Sun, C. Zoufal, R. Iten, N. Shen and S. Woerner. Option pricing using quantum computers. arXiv: 1905.02666, 2019.

[19] J. Vecer. A new PDE approach for pricing arithmetic average Asian options. *Journal of Comp. Finance*, 4: 105-113, 2001.

Lloyds Banking Group plc, Commercial Banking, 10 Gresham Street, London, EC2V 7AE, UK
E-mail address: Filipe.Fontanela@lloydsbanking.com

Department of Mathematics, Imperial College London, and Alan Turing Institute
E-mail address: a.jacquier@imperial.ac.uk

Lloyds Banking Group plc, Commercial Banking, 10 Gresham Street, London, EC2V 7AE, UK
E-mail address: Mugad.Oumgari@lloydsbanking.com